CST-46

Numerical Simulation for Dynamic Stall of NACA0012 at Low Reynolds Number

Boonlue Sawatmongkhon[1,*]

[1] Combustion Technology and Alternative Energy Research Centre – CTAE, Department of Power Engineering Technology, College of Industrial Technology, King Mongkut's University of Technology North Bangkok, Bangkok, Thailand 10800

*Corresponding Author: boonlues@kmutnb.ac.th

Abstract

Dynamic stall of the NACA0012 airfoil at low Reynolds number is studied via computational fluid dynamics (CFD). The one-equation Spalart–Allmaras turbulence model is applied to the two-dimensional and unsteady flow. The sliding mesh method is used to deal with the oscillating airfoil. Hysteresis lift and drag coefficients of the pitching airfoil are investigated by comparing with published experimental data. Different angles of attack and amplitudes of the pitching airfoil are presented in order to scrutinise the flow phenomena started from leading edge to trailing edge. In the deep-stall regime which the turbulent flow is dominant, the simulations show excellent results. However, when the transition flow tends to dominate the flow (in the light-stall regime), the Spalart–Allmaras turbulence model gives fascinated consequences.

***Keywords**:* Dynamic stall; Low Reynolds number; NACA0012; Spalart-Allmaras turbulence model; Pitching airfoil.

1. Introduction

Dynamic stall is an unsteady, separated, and complex flow phenomenon occurring on pitching bodies, such as airfoils and blades. A good physical understanding of dynamic stall is necessary for helicopter, turbomachinery, and wind turbine applications. When fluid passes over an oscillating airfoil, the transient flow structure may be categorised into three different regimes: attached flow, light stall, and deep stall. The attached flow is valid when the maximum dynamic angle of attack is less than the maximum static angle of attack. Boundary layer can stick on the suction side of the airfoil without separation. As the angle of attack is continuously increased until it exceeds the maximum static angle of attack, the light stall is defined. In this regime, there are boundary layer separation and vortex close to the airfoil leading edge resulting in an increase of the lift force. However, the airfoil stall has not occurred yet. As the angle of attack is raised further, the deep stall is happen. The light and deep stalls are usually recognised as the dynamic stall.

In contrast to static stall, the onset of the airfoil stall for a pitching airfoil can be delayed with the stall angle of attack which is greater than the static angle stall by a notable amount. Once dynamic stall occurs, a more detailed knowledge of this severe phenomenon is important in aspects

of unsteady loads, vibration control, dynamic responses, and noise generation.

As the angle of attack which is abruptly increased passes the static stall angle, a concentrated vortex (also known as a dynamic stall vortex) may develop in the boundary layer close to the airfoil leading edge. The flow around the leading edge of the airfoil plays an important role in the development of the vortex. In a low-Reynolds-number flow, transition from laminar to turbulent characteristic is crucial to the creation of the vortex. This vortex is, in short time later, shed downstream into the wake creating separation on the suction side which causes increase in lift [1]. The size of this increase relies on the strength and position of the vortex. During the downstroke phase of the oscillating cycle, the flow reattachment is noticeable when the angle of attack is sufficiently reduced. As a result, the hysteresis loop of lift, drag, and pitching moment of the pitching airfoil are significantly different from the static airfoil. The hysteresis loop depends on the airfoil shape, the amplitude of oscillation, mean angle of attack, Reynolds number, Mach number, and the reduced frequency of oscillation [2]. The reduced frequency is a dimensionless number which is generally used in aerodynamics to represent the unsteadiness of a system. As the reduced frequency is zero, the system is called as the steady-state aerodynamic system. The system with the reduced frequency between 0 and 0.05 is the quasi-steady aerodynamics. If the reduced frequency is larger than 0.05, the system is classified as the unsteady aerodynamics.

By using both experiments and numerical calculations, the effects of transition and turbulence on dynamic stall onset were investigated by [3]. Different tripping devices were installed at the leading edge of an airfoil to generate transition and turbulent flows. In the transition flow, a leading edge separation bubble, which was fluctuating and moving, was developed during the upper part of the upstroke phase. The bubble led to a vorticity which was quickly convected downstream to form areas of concentrated vorticity. Interestingly, the extra local clockwise and anti-clockwise vorticities were detected in this situation. The extra vorticities were then mixed with the main vorticity stream. In cases of the fully turbulent flow, the overall flow features were very similar with the transition flow. However, the difference from the transition flow was that the flow of vorticity was very smooth and a spreading of extra vorticities was not visible. The authors concluded that the occurring of extra vorticities in the transition flow stabilised the flow at the leading edge, delayed the dynamic stall, and improved force and moment hysteresis loops.

The formation and behaviour of laminar separation on a static low-Reynolds-number airfoil were experimentally studied by using a high-resolution particle image velocity (PIV) technique [4]. At the sufficient angle of attack, the adverse pressure gradient caused the formation of laminar separation bubbles in the boundary layer. Then, these bubbles separated from the suction side of the airfoil adjacent to the leading edge. After this point two circumstances can occur. In one case, the separated laminar boundary layer detached fully and transformed rapidly to turbulent flow by generating unsteady Kelvin-Helmholtz vortex structures. In the other case, the separated lami-

nar boundary layer reattached to the airfoil as a turbulent boundary layer. The measured turbulent kinetic energy distributions revealed that the reattached turbulent boundary layer was much more potential; therefore, it was more capable to resist an adverse pressure gradient without separation (comparing with the laminar boundary layer located at upstream of the separation bubble). The size of the laminar separation bubble was about 20% of the airfoil chord length. This size was almost unchanged with the angle of attack.

The objective of this paper is to investigate the dynamic stall of the NACA0012 airfoil oscillating under the low-Reynolds-number flow. Hysteresis loops of aerodynamic forces will be studied by comparing with experimental data. Furthermore, notice about limitation of a turbulence model (the one-equation Spalart-Allmaras turbulence model is employed in this paper) is given. Moreover, suggestions to improve understanding of the low-Reynolds-number dynamic stall are also provided.

2. Methodology

In this paper, a numerical simulation is introduced to investigate the underlying physics of the dynamic stall. The well-known NACA0012 airfoil with the chord length 0.15 m was continuously oscillated with sinusoidal angles of attack. The pitching axis was located at the middle of the airfoil chord length. The harmonic angles of attack (α) were controlled by the function

$$\alpha(t) = \alpha_0 + \alpha_1 \sin(\omega t) \quad (1)$$

where α_0 is the mean angle of attack; α_1 is the amplitude of the harmonic oscillation; ω is the frequency of the oscillation; and t is the instantaneous time. The frequency of the oscillation can be estimated from the definition of the reduced frequency (k)

$$k = \frac{\omega c}{2U_\infty} \quad (2)$$

where c is the airfoil chord length and U_∞ is the freestream velocity. With U_∞ = 14 m/s and the reduced frequency k = 0.1, the corresponding frequency of the oscillation is 18.67 rad/s. Seven oscillating profiles studied in this paper are listed in Table 1. Only pitching airfoil is considered in this paper. The plunging movement is not studied in this phase. The Reynolds number based on the chord length is around 1.35×10^5.

Table 1 Angle of attack configurations

Deep stall	Light stall
α = 5° + 15° sin(ωt)	α = 0° + 15° sin(ωt)
α = 10° + 15° sin(ωt)	α = 5° + 10° sin(ωt)
α = 15° + 10° sin(ωt)	α = 10° + 5° sin(ωt)
α = 15° + 15° sin(ωt)	

An O-grid type was created by using the grid generation software GAMBIT® with the generally accepted far-field boundary 10 times of the chord length. The sliding mesh module which was incorporated with ANSYS FLUENT® was employed in order to imitate the cyclical motion of the airfoil. The 51200 elements O-grid domain was divided into two zones. The outer zone was stationary while the inner zone can be controllably slid via a user defined function (UDF) subroutine of the FLUENT. The grid distribution was forced to be high resolution in the region close to the airfoil surface. The distance of the first elements next to the airfoil surface was set to correspond to $y^+ < 1$. Fig. 1 illustrates the computational domain which is employed to numerically simulate in this study.

Regarding computational cost, the two-dimensional unsteady Reynolds-averaged Navier-Stokes equations (URANS) together with the one-equation Spalart-Allmaras turbulence model were selected to elucidate complex phenomena of the dynamic-stall flow. The Spalart-Allmaras turbulence model was designed especially for aerospace applications; it solves a modelled transport equation for kinematic eddy viscosity without calculating the length scale related to the shear layer thickness [5]. According to [3], the Spalart-Allmaras turbulence model provided the most accurate results for problems of dynamic stall.

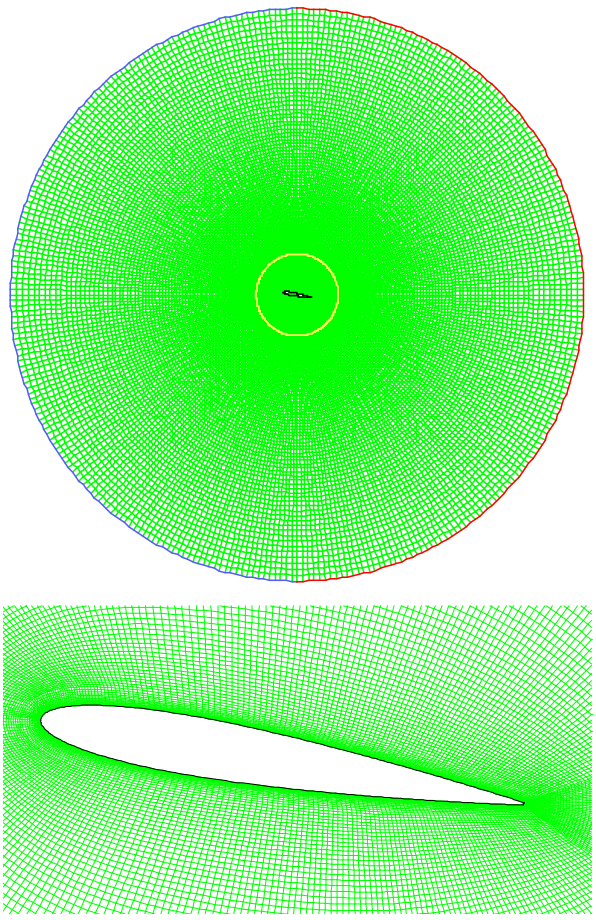

Fig. 1 Illustration of the O-grid computational domain

The most popular two-equation k-ε turbulence model is avoided in this paper because it performs poorly for complex flows involving severe pressure gradient and separation [6].

The initial flow field for the unsteady simulation was prepared by applying the calculation of the steady-state configuration when the airfoil was positioned at the mean angle of incidence. Next, the unsteady calculation was carried on until periodic monitored solutions (e.g. lift and drag coefficients) were achieved; and then the calculation process was stopped.

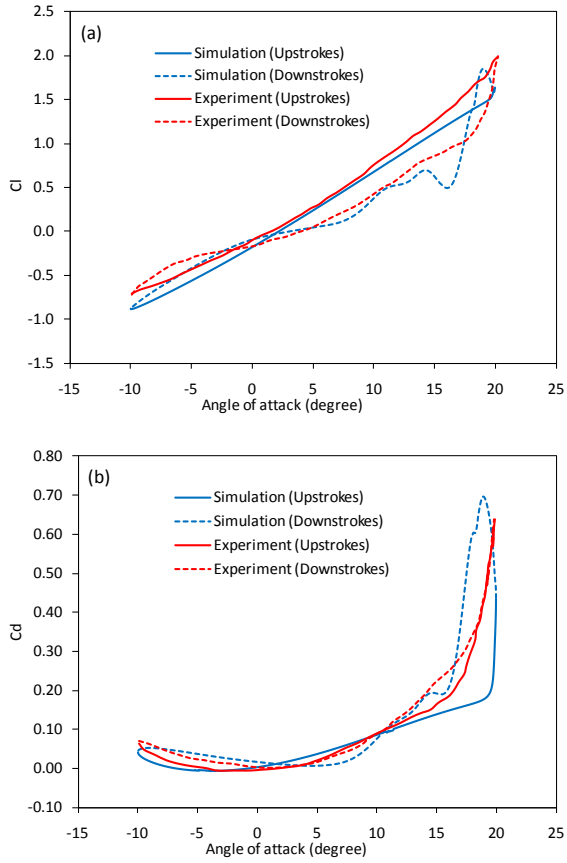

Fig. 2 Hysteresis loops of lift and drag coefficients; $\alpha = 5° + 15° \sin(\omega t)$; (a) Lift coefficient; (b) Drag coefficient

3. Results and Discussions

Aerodynamic coefficients, lift coefficient (C_l) and drag coefficient (C_d), computed by the numerical simulation are compared with experimental data published by [7]. The results are organ-

ised into two distinct regimes: deep stall and light stall.

3.1 Deep-Stall Regime

Four cases of the deep stall are presented in Fig. 2 – Fig. 5. The maximum angle of attack for each deep-stall case considerably exceeds the static stall angle of attack (approximately 13° for NACA0012). So, the flow field is extremely complex and the flow structure is reasonably classified as fully turbulence. As seen in Fig. 2, the lift and drag coefficients from the simulation are readily agreed with the experiments. Fig. 2b shows that the effect of unfavourable drag force is obviously noticeable when the angles of incidence are over the static stall angle of attack.

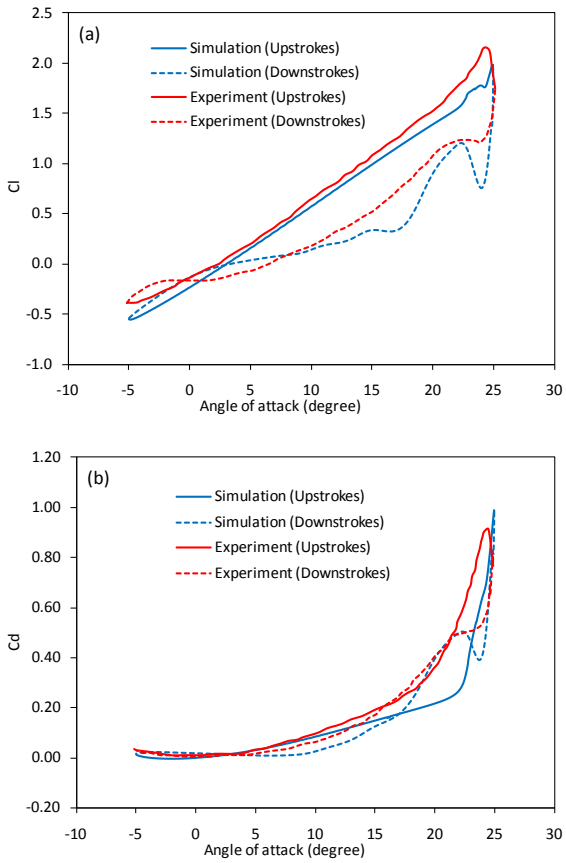

Fig. 3 Hysteresis loops of lift and drag coefficients; $\alpha = 10° + 15° \sin(\omega t)$; (a) Lift coefficient; (b) Drag coefficient

In cases of the results given in Fig. 3 and Fig. 4, although the peak angle of attack is identical (25°), the differences in the mean angle of attack and the amplitude of oscillation cause the unequal aerodynamic responses.

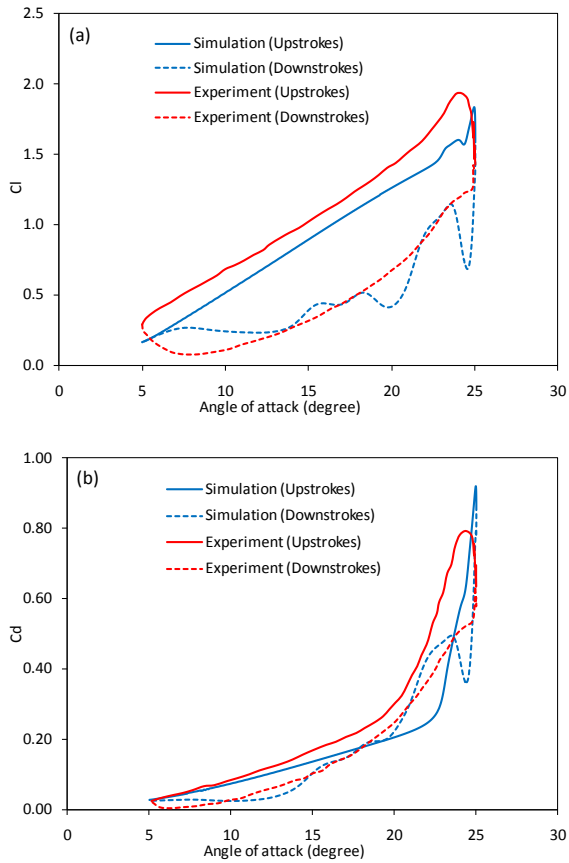

Fig. 4 Hysteresis loops of lift and drag coefficients; $\alpha = 15° + 10° \sin(\omega t)$; (a) Lift coefficient; (b) Drag coefficient

At a constant reduced frequency, an oscillating airfoil with the higher amplitude moves angularly faster than that with the lower amplitude. This means that the airfoil in Fig. 3 oscillates quicker than the airfoil in Fig. 4. The faster oscillating airfoil gives the relatively narrow hysteresis loop of lift as can be seen that the upstroke and downstroke of the lift coefficient are relatively closer. The simulation shows fluctuations in the lift coefficient as the airfoil is in the downstroke cycle. In

contrast, the fluctuation is not found in the upstroke phase. The fluctuations in hysteresis loops of lift and drag coefficients were also detected even when the more sophisticated SST k-ω turbulence model was obtained [8]. In terms of the drag coefficient, the simulation gives underprediction results, for both pitching patterns, during the upstroke cycle. During the downstroke, fortunately, the simulation can provide the qualitatively and quantitatively acceptable results.

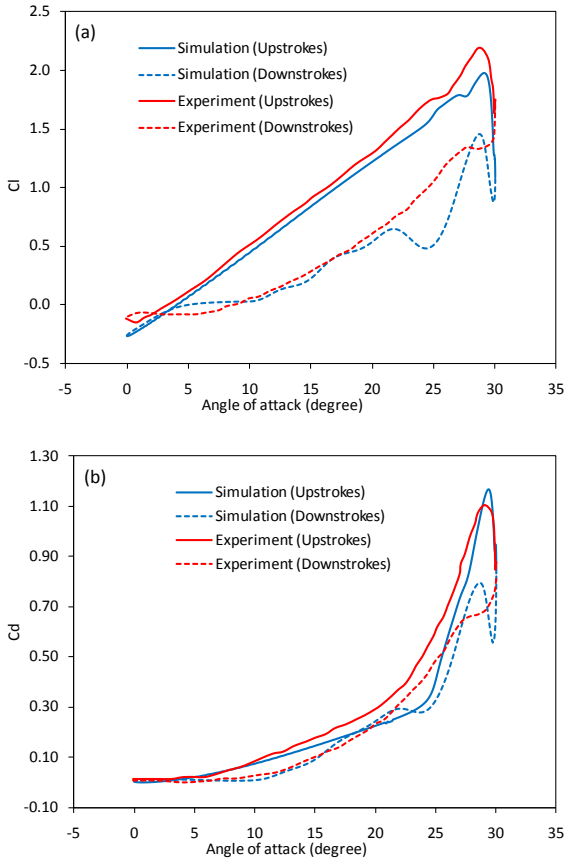

Fig. 5 Hysteresis loops of lift and drag coefficients; $\alpha = 15° + 15° \sin(\omega t)$; (a) Lift coefficient; (b) Drag coefficient

Fig. 5 presents the calculation at the largest both the mean angle of attack and the amplitude of oscillation. Both aerodynamic coefficients are quite satisfying with the experimental data. Physical phenomena can be vividly captured by the CFD. The fluctuation of lift coefficient is still observed at the initial part of the downstroke cycle. Compared with the case shown in Fig. 4 where the mean angle of attack is identical, Fig. 5 shows the narrower hysteresis loop of lift coefficient because its angular movement is quicker.

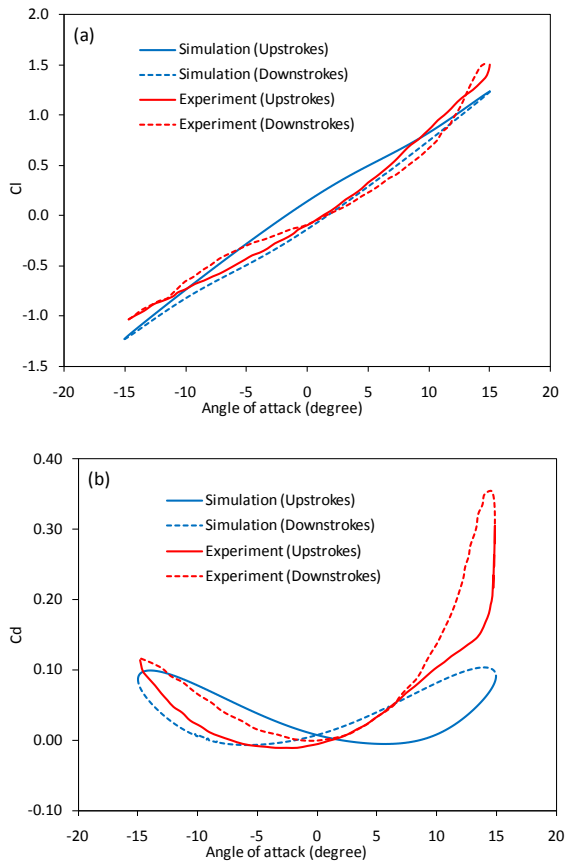

Fig. 6 Hysteresis loops of lift and drag coefficients; $\alpha = 0° + 15° \sin(\omega t)$; (a) Lift coefficient; (b) Drag coefficient

3.2 Light-Stall Regime

The flow field around a pitching airfoil is predominantly characterised by the degree of separation. Due to high extent of separation, the flow structure in the deep-stall regime is naturally assumed to be the fully turbulent flow, so that the Spalart-Allmaras turbulence model can provide very good results. In contrast, as the flow is in the

light-stall regime, laminar to turbulent transition may play an important role for low-Reynolds-number flows. This makes the Spalart-Allmaras turbulence model unable to realise flow characteristic caused by the transitional effect.

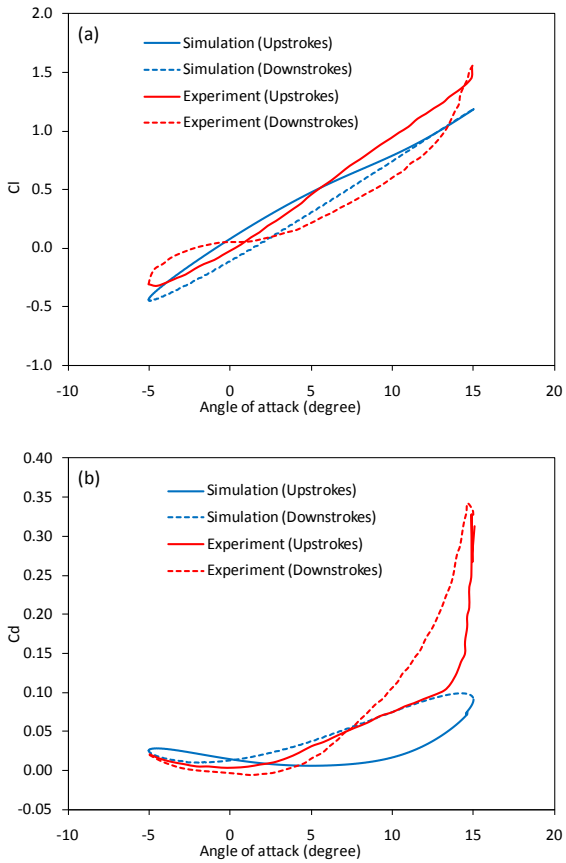

Fig. 7 Hysteresis loops of lift and drag coefficients; $\alpha = 5° + 10° \sin(\omega t)$; (a) Lift coefficient; (b) Drag coefficient

Results of the calculation in the light-stall class are compared with experiments as illustrated in Fig. 6 – Fig. 8. The maximum angles of attack of these three cases are all equal to 15°. Fig. 6 and Fig. 7 reveal that the Spalart-Allmaras turbulence model can be utilised to predict the hysteresis loop of lift coefficient. However, the turbulence model fails to provide information about drag coefficient when, especially, angles of attack exceed their mean angles of attack. Accordingly, there is a cautious conclusion that, in the light-stall regime, the unacceptable hysteresis loop of the drag coefficient is produced when the Spalart-Allmaras turbulence model is applied.

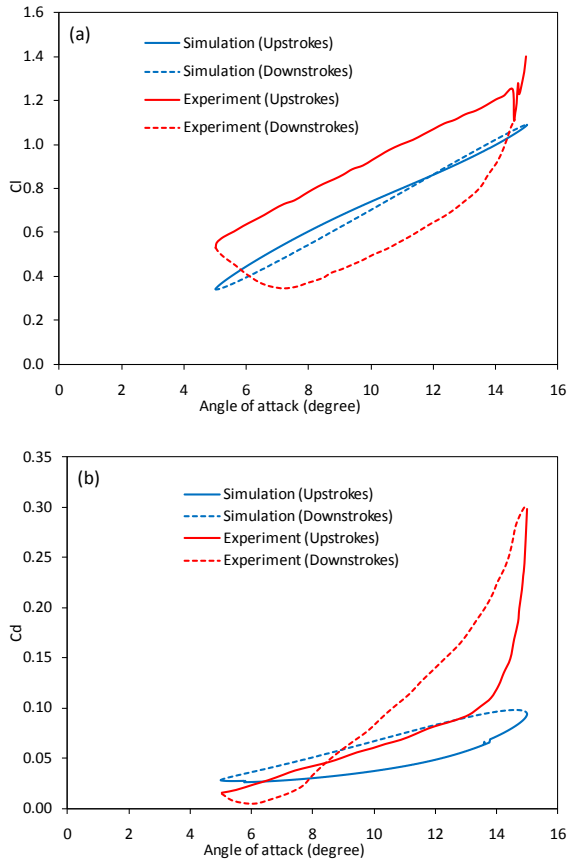

Fig. 8 Hysteresis loops of lift and drag coefficients; $\alpha = 10° + 5° \sin(\omega t)$; (a) Lift coefficient; (b) Drag coefficient

Interestingly, the case shown in Fig. 8 represents the slowest movement of the airfoil (the smallest amplitude of oscillation). Thus, the complexity and generation of turbulence in this case may be limited which result in the flow structure be dominated by the laminar to turbulent transition or even by the laminar flow rather than the turbulent flow. As a result, the Spalart-Allmaras turbulence model yields the incorrect hysteresis loops of both lift and drag coefficients. It seems like that the simulation is unable to predict the

existence of airfoil dynamic stall. In order to deal with this challenge, different laminar to turbulent transition models, such as suggested by [9,10,11], may be obtained to elucidate the dynamic-stall flow in the light-stall regime.

4. Conclusions

The oscillating NACA0012 airfoil in a flow with low Reynolds number was investigated by using the CFD. Underlying dynamic stall causes substantial rise in lift and drag forces. The one-equation Spalart–Allmaras turbulence model gives reasonable hysteresis loops of lift and drag coefficients when the airfoil is under the flow dominated by turbulence (the deep-stall regime). However, the Spalart–Allmaras turbulence model shows unacceptable predictions in the light-stall regime. Presumably, the effect of the transition from laminar to turbulent flow is crucial in this regime. For that reason, the Spalart–Allmaras turbulence model, which works efficiently in the fully turbulent circumstance, should be avoided when the flow studied is in the light-stall regime. A laminar to turbulent transition model may be considered to cope with this difficulty.

7. References

[1] Ekaterinaris, J. A. and Platzer, M. F. (1997). Computational prediction of airfoil dynamic stall, *Progress in Aerospace Sciences*, vol. 33 (11-12), pp. 759-846.

[2] Barakos, G. N. and Drikakis, D. (2003). Computational study of unsteady turbulent flows around oscillating and ramping aerofoils, *International Journal for Numerical Methods in Fluids*, vol. 42, pp. 163-186.

[3] Geissler, W. and Haselmeyer, H. (2006). Investigation of dynamic stall onset, *Aerospace Science and Technology*, vol. 10, pp. 590-600.

[4] Hu, H. and Yang, Z. (2008). An experimental study of the laminar flow separation on a low-Reynolds-number airfoil, *Journal of Fluids Engineering*, vol. 30, pp. 051101-1 - 051101-11.

[5] Spalart, P. R. and Allmaras, S. R. (1992). A one-equation turbulence model for aerodynamic flows, *AIAA*, no. 92-0439.

[6] Menter, F. R. (1994). Two-equation eddy-viscosity turbulence models for engineering applications, *AIAA Journal*, vol. 32, no. 8, pp. 1598-1605.

[7] Gerontakos, P. (2004). An experimental investigation of flow over an oscillating airfoil, Master thesis, *McGill University*, Montreal, Quebec, Canada.

[8] Wang, S., Ingham, D. B., Ma, L., Pourkashanian, M. and Tao, Z. (2010). Numerical investigations on dynamic stall of low Reynolds number flow around oscillating airfoils, *Computers & Fluids*, vol. 39, pp. 1529-1541.

[9] Walters, D. K. and Cokljat, D. (2008). A three-equation eddy-viscosity model for Reynolds-averaged Navier–Stokes simulations of transitional flow, *Journal of Fluids Engineering*, vol. 130 (12), pp. 121401(1)-121401(14).

[10] Suluksna, K., Dechaumphai P. and Juntasaro, E. (2009). Correlations for modeling transitional boundary layers under influences of freestream turbulence and pressure gradient, *International Journal of Heat and Fluid Flow*, vol. 30, pp. 66-75.

[11] Juntasaro, E. and Ngiamsoongnirn, K. (2014). A new physics-based γ–k_L transition model, *International Journal of Computational Fluid Dynamics*.